

Demonstration of a radio-frequency spectrum analyzer based on spectral hole burning

Loïc Ménager, Ivan Lorgéré, and Jean-Louis Le Gouët

Laboratoire Aimé Cotton, Centre National de la Recherche Scientifique II, Bâtiment 505, 91405 Orsay Cedex, France

Daniel Dolfi and Jean-Pierre Huignard

Laboratoire Central de Recherche, Thomson-CSF, Domaine de Corbeville, 91404 Orsay Cedex, France

Received February 26, 2001

Spectral hole-burning (SHB) technology is considered for >10 -GHz instantaneous bandwidth signal-processing applications. In this context we report on what is believed to be the first demonstration of a SHB microwave spectrometer. A set of gratings engraved in a SHB crystal is used to filter one sideband of the optically carried microwave signal. The setup is confined to narrow-bandwidth operation, over a 35-MHz-wide interval. The first findings confirm the validity of the architecture in terms of spectral resolution, angular channel separation, and simultaneous detection of multiple spectral lines. © 2001 Optical Society of America

OCIS codes: 020.1670, 070.1670, 300.6240, 300.6370, 350.4010.

Much attention has been dedicated to far-infrared and submillimeter spectroscopy in recent or planned space observatories.¹ In a submillimeter system the input signal undergoes frequency downshifting before it reaches the back-end spectral analyzer. The latter exhibits an instantaneous bandwidth of several tens of gigahertz. We report what we believe is the first experimental demonstration of a radio-frequency (rf) spectrum analyzer based on spectral hole burning (SHB). The ultimate goal of this investigation is to devise a rf spectrometer with a bandwidth in excess of 10 GHz and with more than 1000 simultaneous spectral channels.

Efforts to promote SHB technology have long been focused on large-capacity data storage applications. Competition with well-established technology proved unsuccessful. SHB technology is more likely to emerge in the field of optical processing because it offers outstanding performance in terms of bandwidth and time–bandwidth product. Various optical functions, such as time-domain correlation,^{2,3} real-time data routing,^{4,5} and true-time delay generation for radar application,⁶ were demonstrated recently that illustrate the signal-processing potential of SHB. However, cryogenic requirements drastically limit the domains where a SHB solution is practicable. The cooling capabilities of some recently launched space observatories meet the needs of the novel application that we demonstrate.

The SHB spectrometer concept relies on the engraving of monochromatic gratings in a rare-earth-ion-doped crystal. This set of gratings is used to filter (see Fig. 1) one of the sidebands of an optically carried microwave signal. This microwave signal is normally transferred onto the optical carrier by an electro-optic Mach–Zehnder modulator (MZM), and the modulated beam is directed to the SHB spectrometer. By fortunate coincidence, the bandwidth of the SHB medium matches that of integrated MZMs developed for high-data-rate telecommunication. In our present initial demonstration, however, we are limited to the 35-MHz bandwidth of the acousto-optic modulators (AOM) we had at our disposition.

Resonant optical excitation of the atomic ions embedded in the rare-earth-ion-doped crystal brings about spectrally selective reduction of absorption. This is the essence of SHB. As the hole depth is proportional to the burning intensity, the interference pattern of two monochromatic angled beams inscribes an absorption grating that is able to diffract an incident probe beam. Such a grating diffracts a single spectral component with a resolution that is ultimately determined by the homogeneous linewidth of the SHB medium, which is usually less than 1 MHz at a temperature of 5 K. A large number of gratings can coexist within the inhomogeneous width of the absorption line, which may reach tens of gigahertz. By varying the laser frequency in synchrony with the angle of incidence during the engraving procedure, one associates a specific diffraction angle with each specific spectral component. Therefore the different spectral components of an incident polychromatic probe beam are diffracted and simultaneously retrieved in different directions. The stack of monochromatic

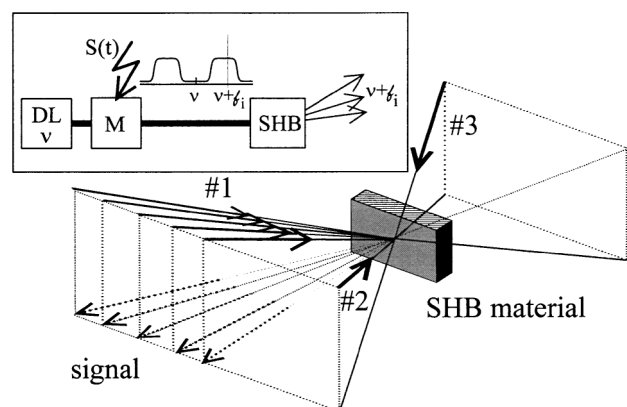


Fig. 1. Overall beam arrangement, with the spectrometer principle shown in the inset. The modulator (M) transfers the rf signal $S(t)$ onto the monochromatic carrier delivered by the laser (DL). Carrier frequency ν combines with the rf components at frequency f_i in the two sidebands. Each component at frequency $\nu + f_i$ is diffracted in a specific direction by the gratings engraved upon the SHB plate.

gratings works as a spectrometer that is expected to exhibit a resolution of less than 1 MHz and a bandwidth of several tens of gigahertz. The connection between the engraving laser's incidence angle and the laser frequency is essentially arbitrary. Therefore, by reducing the engraving laser's frequency-tuning range while the angular scanning range is kept fixed, one actually zooms in on a specific spectral region that is analyzed with improved resolution. The spectral selectivity of hole burning is inherently local and differs strongly from the conventional Bragg selectivity of holograms engraved by counterpropagating beams, which depends on the sample's thickness.

The spectrum analyzer involves two engraving beams and a readout beam, which are numbered #1, #2, #3, respectively. The rf signal to be analyzed is carried by the readout beam. The counterpropagating noncoplanar arrangement is summarized in Fig. 1. The frequency-selective deflection of one engraving beam and the corresponding fanning out of the diffracted readout beam are also represented in this figure. The three beams are split from a single, fixed-frequency laser source. The required angular and frequency scans of the engraving beams are achieved by AOMs in the present demonstration. Whereas the deflector placed on beam #1 simultaneously affects the wave-vector direction and the optical frequency, the AOM on beam 2 acts mainly as a frequency shifter, with little effect on the direction of the wave vector. To keep the beams focused on the same slab spot while the AOM frequency is varied, one sets the AOM in imaging position with respect to the sample with the help of two-lens optical relays.

Let w represent the engraving beam's diameter inside the SHB slab. A monochromatic probe beam is diffracted by the engraved grating in a specific frequency-dependent direction with the diffraction-limited angular resolution $\delta\varphi = \lambda/w$. Let $\Delta\varphi$ denote the angular range of the acousto-optic deflector when the acoustic frequency is varied over a bandwidth of $\Delta\nu$. The finite angular width of the diffracted beam results in a spectral resolution of $\delta\nu = \delta\varphi(\Delta\nu/\Delta\varphi)$.

We performed the experiment with a 2.5-mm-long Tm^{3+} :YAG crystal (0.5 at. %) maintained at 5 K in a helium cryostat (see Fig. 2). The three beams are split from the continuous-wave output of a laser diode that is resonant with the 793-nm transition of Tm^{3+} . The homogeneous width is ~ 150 kHz, and the inhomogeneous width exceeds 20 GHz. The AOM deflector and shifter chirp the engraving beam's frequency at the rate of 4.1×10^{12} Hz s^{-1} over a $\Delta\nu = 35$ MHz bandwidth, simultaneously scanning the beam angle over a $\Delta\varphi = 80$ mrad range. The 4-mW engraving beams are focused onto a 200- μm -diameter spot, which leads to $\delta\varphi = 4$ mrad and $\delta\nu = 1.5$ MHz. The channel width is actually limited by the laser frequency fluctuations that take place during the 10-ms engraving accumulation time rather than by diffraction. The SHB gratings are stored in the ions excited to the transition upper level, 3H_4 . They are rapidly erased by spontaneous decay to the ground level, 3H_6 . Therefore the inscribed diffraction gratings must be continually refreshed. Decay to the ground level is

actually slowed down by intermediate shelving level 2F_4 , whose lifetime is ~ 10 ms. With an engraving repetition rate of 2 kHz, one expects less than a 10% drop in the diffraction efficiency between refreshes. The modulated probe beam is directed to the Tm^{3+} :YAG crystal and is diffracted by the engraved gratings in a frequency-dependent direction. The angular separation of the signal from all other beams is achieved in a phase-matched condition with the help of a noncoplanar⁷ beam arrangement (see Fig. 1). The emerging signal is directed to a 1024-pixel photodiode array (PDA; Fig. 2) located in the focal plane of a lens. The pixels are 2.5 mm high by 25 μm wide. The illuminated position coordinate on the PDA is proportional to the deflection angle and thus to the rf of the signal. The diode array can be read out in a little more than 5 ms, which represents the minimum integration time. The array is integrated continuously; the pixels are read out sequentially and collect photons again immediately after readout. The array readout is not synchronized with the rf signal sequence. Without further improvement the detection is not immune to stray light. Specifically, the PDA collects the light scattered from the cryostat windows. To filter out this unwanted background we image the active region of the sample onto a pinhole with the help of an optical relay. In this way the emitting area is precisely located. This procedure appears to be highly efficient in rejecting stray light produced by the engraving beams. However, it is not sufficient to completely eliminate stray light from the probe beam. We therefore resort to polarization selection with cross-polarized engraving beams. The detection polarizer is then also crossed with respect to the polarization of the probe beam.

In a first demonstration, a single-frequency rf signal was superimposed onto probe beam #3. The rf signal was composed of short pulses, a few microseconds long, that were fed to the AOM in synchrony with the engraving pulses. In a realistic application this AOM would be replaced with a fast MZM. The PDA signal is displayed in Fig. 3. Vertical lines delimit the

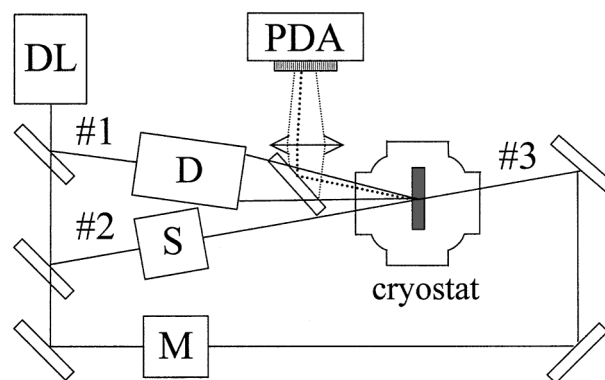


Fig. 2. Experiment setup. A diode laser (DL) delivers the beams #1, #2, and #3. An acousto-optic deflector (D) and shifter (S) control the engraving beams. The rf signal is transferred onto the optical carrier with the help of a modulator (M). In a realistic application M is a MZM. In the experiment, M is an AOM. The deflected beam is detected on a photodiode array (PDA).

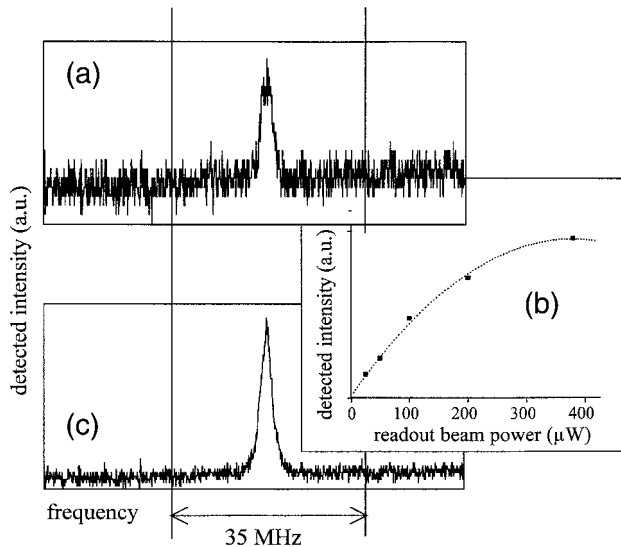


Fig. 3. Spectral analysis of a single-frequency rf signal as detected on the PDA. The profile does not broaden when the probe beam power is varied from $25 \mu\text{W}$ in (a) to $770 \mu\text{W}$ in (c). The duration of the signal pulse is $10 \mu\text{s}$. The detected intensity saturation as a function of the probe beam power is shown in (b).

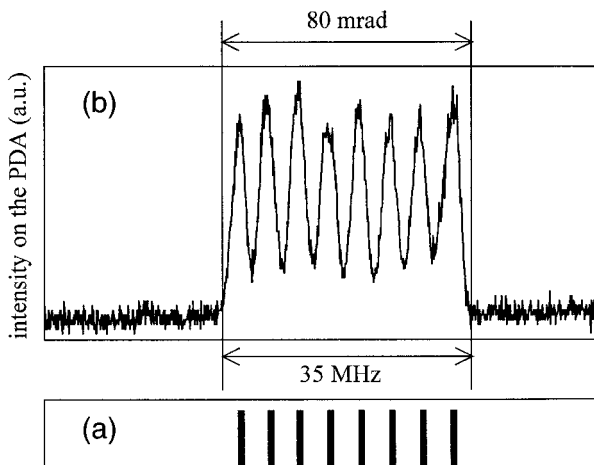


Fig. 4. (b) Spectral analysis of (a) an eight-component rf signal. The deflection angle of the detected beam is proportional to the rf shift.

detection window. As expected, the observed spectral width slightly exceeds the 1.5-MHz diffraction limit. An important feature of the setup is the absence of line broadening when the signal intensity is varied. Excessive signal intensity results only in the saturation of the response amplitude but does not affect the linewidth, as illustrated in Fig. 3, where Figs. 3(a) and 3(c), respectively, correspond to probe beam powers of 25 and $770 \mu\text{W}$. One spectral channel was spread over 50 pixels. Focusing each channel onto a single pixel would result in better sensitivity and dynamic range. In a second experiment we simulated a comb

spectrum by making the probe field undergo a 4-MHz shift every $2 \mu\text{s}$ during a $16\text{-}\mu\text{s}$ interval. Thus eight evenly spaced lines occupied a 33-MHz interval [see Fig. 4(a)]. The corresponding PDA signal is displayed in Fig. 4(b). The linewidth was not affected by the presence of several components.

The present duty cycle of the engraving step is only 1.7%. A 100% duty cycle device should span 2 GHz, with the same diffraction efficiency, under identical conditions of laser intensity, active area size, refresh rate, and chirp rate. Indeed, the different monochromatic gratings are built from different independent active atoms. For such large-bandwidth operation we should scan the engraving laser frequency over several gigahertz, in synchrony with the acousto-optic deflector, with the high degree of repeatability required for accumulated storage.

In summary, the operating principle of a spectral hole-burning microwave spectrometer that uses optically carried microwave signals has been described. A preliminary experimental demonstration was presented that yielded a resolution of 2.5 MHz, in good agreement with theory. The use of AOMs for optical frequency scan and microwave signal modulation of the carrier has resulted in the present 35-MHz bandwidth limitation, but the bandwidth of the available active material exceeds 20 GHz. A broadband demonstration and large channel number operation are anticipated. A wider bandwidth should be feasible through direct tuning of the laser cavity length and fast MZM signal transfer onto the carrier. An appropriate laser cavity has been developed.⁸ To increase the channel number, one can resort to a bidirectional deflection pattern.

We are grateful to the European Space Agency for continuing support provided under contracts ESA 12876/98/NL/MV and ESTEC 14174/00/NL/SB. J. L. Le Gouët's e-mail address is jean-louis.legouet@lac.u-psud.fr.

References

1. E. F. van Dishoek and F. P. Helmich, in *Proceedings of the 30th ESLAB Symposium on Submillimetre and Far-Infrared Space Instrumentation*, E. J. Rolfe, ed., ESA SP-388 (European Space Agency, Munich, Germany, 1996), pp. 3–12.
2. T. L. Harris, Y. Sun, W. R. Babbitt, R. L. Cone, J. A. Ritcey, and R. W. Equall, *Opt. Lett.* **25**, 85 (2000).
3. M. Tian, F. Grelet, I. Lorgeré, J. P. Galaup, and J.-L. Le Gouët, *J. Opt. Soc. Am. B* **16**, 74 (1999).
4. T. Wang, H. Lin, and T. W. Mossberg, *Opt. Lett.* **20**, 2541 (1995).
5. T. L. Harris, Y. Sun, R. L. Cone, R. Macfarlane, and R. W. Equall, *Opt. Lett.* **23**, 636 (1998).
6. K. D. Merkel and W. R. Babbitt, *Opt. Lett.* **23**, 528 (1998).
7. J. A. Shirley, R. J. Hall, and A. C. Eckbreth, *Opt. Lett.* **5**, 380 (1980).
8. L. Ménager, L. Cabaret, I. Lorgeré, and J.-L. Le Gouët, *Opt. Lett.* **25**, 1246 (2000).